X-ray diffraction enhanced imaging study of intraocular tumors in human beings*

TAN Gao(谈高)[1,2,3] WANG Hua-Qiao(汪华侨)[1;1)] CHEN Yu(陈雨)[4] YUAN Qing-Xi(袁清习)[4] LI Gang(黎刚)[4] ZHANG Xiao-Dan(张晓丹)[5] ZHU Pei-Ping(朱佩平)[4] ZHONG Xiu-Feng(钟秀风)[6] TANG Jin-Tian(唐劲天)[3;2)]

[1] Department of Anatomy and Brain Research, Biomedical Engineering Center, Zhongshan School of Medicine, Sun Yat-sen University, Guangzhou 510080, China

[2] The Fifth Affiliated Hospital of Sun Yat-sen University, Zhuhai 519000, China

[3] Key Laboratory of Particle & Radiation Imaging, Education Ministry of China, Department of Engineering Physics, Tsinghua University, Beijing 100084, China

[4] Institute of High Energy Physics, Chinese Academy of Sciences, Beijing 100049, China

[5] The First Affiliated Hospital of Tsinghua University, Beijing 100016, China

[6] The State Key Laboratory of Ophthalmology, Zhongshan Ophthalmic Center, Sun Yat-sen University, Guangzhou 510080, China

Abstract Diffraction enhanced imaging (DEI) with edge enhancement is suitable for the observation of weakly absorbing objects. The potential ability of the DEI was explored for displaying the microanatomy and pathology of human eyeball in this work. The images of surgical specimens from malignant intraocular tumor of hospitalized patients were taken using the hard X-rays from the topography station of Beamline 4W1A at Beijing Synchrotron Radiation Facility (BSRF). The obtained radiographic images were analyzed in correlation with those of pathology. The results show that the anatomic and pathologic details of intraocular tumors in human beings can be observed clearly by DEI for the first time, with good visualization of the microscopic details of eyeball ring such as sclera, choroids and other details of intraocular organelles. And the best resolution of DEI images reaches up to the magnitude of several tens of μm. The results suggest that it is capable of exhibiting clearly the details of intraocular tumor using DEI method.

Key words diffraction enhanced imaging (DEI), intraocular malignant tumor, synchrotron radiation, X-ray phase-contrast imaging (XPCI), X-ray absorption contrast imaging (XACI)

PACS 87.59.-e

1 Introduction

It is well known that the X-ray radiography works well in distinguishing hard and soft tissues, but with great difference in the attenuation of X-rays. Even for the intermediate differences of absorption between tissues such as muscle and fat, their distinction can also be provided with an X-ray CT scan. However, problems arise when the organic matter is made mainly only of weakly absorbing carboniferous objects such as C, H, O and N, etc. These problems are often encountered in medical sciences. In this paper, such problems are investigated.

Because of their low contrast differences, most of the medical soft tissues cannot be seen to any extent with the X-ray absorption contrast imaging (XACI) methods mentioned above. Although the other types of modern medical imaging methods can provide important information on human internal structures than XACI, such as ultrasonic and MRI techniques, these methods still suffer from a limited resolution [1].

Received 14 April 2009, Revised 11 August 2009

* Supported by National Natural Science Foundation (10490195), Key Project of Chinese National Programs for Fundamental Research and Development (973 program) (2006cb500700), Natural Science and Technology Foundation of Guangdong Province (04009356, 2008B030301320)

1) Corresponding Author: WANG Hua-qiao, Professor; PhD. Tel: +86-020-87332218; E-mail: wanghq@mail.sysu.edu.cn

2) Corresponding Author: TANG Jin-tian, Professor; PhD. Tel: +86-010-62796769; E-mail: tangjt@mail.tsinghua.edu.cn

Recently, some novel X-ray imaging techniques based on the X-ray phase contrast imaging (XPCI) are developed [2–5]. With the emergence of the third generation of synchrotron radiation facilities, the study related to XPCI has become quite active [6–10], hence the new notion of micro-imaging (resolution <1 mm) is introduced.

Rather than XACI which detects the absorption of X-rays, XPCI detects the phase shifts inside soft tissue [7] which induces the contrast based on the refractive index and then enhances the visibility of the edges between the regions with different refractive indexes. With this new mechanism its resolution has reached the magnitude of tens of μm and the information of subtle changes of internal structure in soft tissue can be obtained three orders of magnitude (1000 times) higher than that of XACI [5, 10]. As one of the XPCI methods, the X-ray diffraction enhanced imaging method (DEI) is based on the fact that refraction distorts the phase front of the X-ray wave transmitted through the object. X-ray wave will deflect from its initial direction by small angles, which depend on the spatial distribution of the mass density [5, 7]. Although there is a small density gradient, the DEI technique visualizes the internal structure of a weakly absorbing object with a high spatial resolution [7, 11–13]. For this reason, after the relevant fundamental theory was first completed by Chapman et al in 1997 [3–5], more and more imaging study with DEI in different aspects such as breast, cartilage and lung tissue, etc., has already been reported [6–10].

Eyeball is a kind of typical soft tissue consisting mostly of low Z lighter elements. So far, the observation of eyeball in ophthalmology mainly relies on Ultrasound and MRI. Both of the two methods belong to the macro-imaging due to their relatively low spatial resolution (⩾1 mm). Thus, the intraocular diseases are usually only detected at far advanced stages. Lack of imaging quality or resolution practically with respect to eyeball is obviously the prime reason for this unfortunate situation.

In 2007, the imaging of porcine eye specimens by the DEI with SR was reported by M. Kelly et al [11]. In their experiments no important anatomic details were shown by XACI, but instead , the contrast resolution of 100 μm was reached by DEI, and the different layers of eye ring were observed. In 2008, a specimen of another ophthalmologic disease, corneal sequestrate of a Persian cat in this case, was investigated with DEI by a group of Brazilian scientists [12]. It proved that the DEI is useful to identify different structures in healthy and diseased (with cataract) crystalline lenses. Micro calcifications were also found in experiment developed with X-ray of higher energies.

In this paper, the imagings of human eyeball and tumors originating from it are performed using DEI method for the first time. The results show good visualization of the great microscopic details with 40 μm resolution of eyeball ring such as sclera, choroids and other details of intraocular organelles. The comparisons between XACI and the DEI contrast are made through experiment and analyses. And some factors with which the image quality would be affected or interrelated in the eyeball imaging of human beings are discussed.

2 Experiment

7 surgical pathology specimens of human intraocular malignant tumors from 4 hospitalized patients were imaged with DEI in this work under agreement with written informed consent from all patients: All of the specimens were fixed in formalin solution [dilute formaldehyde (1:10), mixed with buffering solution (pH 7.0)] and preserved in small tubes under room temperature. Before the DEI experiments, the specimen blocks were cut to about 12 (long) ×9 (high or wide) ×(2–5) mm (thick) in size because of the limited area of imaging detector. The specimens were exposed to air about 15 minutes to dry somewhat and then were put in plastic bags which could be easily penetrated by X-rays .

The DEI experiment was performed at the Topography Sation of Beamline 4W1A at BSRF. The DEI system consisted of two Si(333) crystals fixed in Bede diffractometer accurately, acting as monochromator and analyzer respectively. The specimen to be observed was put between these two crystals. The principle of the DEI technique was given in Ref. [4]. The function of the first crystal (monochromator) is to obtain specific X-rays with an energy of approximately 15 keV, and the monochromatic X-ray is then incident on the specimen. The second crystal (analyzer) is used to distinguish the tiny refracted X-rays caused by the density gradient distribution in the specimen. The X-rays emerging from the sample and hitting the analyzer crystal will satisfy the conditions for Bragg diffraction only within a very narrow window of incident angles, typically on the order of a few μrad. With such an arrangement, even a small variation in the angle of incidence of X-rays on the analyzer significantly changes the diffracted intensity [5–7]. The diffracted X-ray beam out from the analyzer was detected by an X-ray CCD camera with 1300 pixels×1030 pixels and pixel size of approximately 10.9×10.9 μm (X-ray FDI-18 mm camera system, Photonic Science Ltd, UK). The exposure time in the DEI experiment was selected between about 0.05–0.10 seconds according to the energy of X-ray and slightly different from the specimens due to the difference in the thickness of them.

The amount of intensity which passes the analyzer without specimen at a given tuning angle is described as the background data of rocking curve (RC) [7, 10]. When the analyzer is perfectly aligned with the monochromator, say at the top of the RC, it will filter out any X-rays that are scattered or refracted by more than a few μrad. When the analyzer is mis-oriented at a small angle with respect to the monochromator, for example at the half-maximum in the left or right side of the RC (±0.5 FWHM), then the X-rays refracted by a smaller angle will be reflected less, and the X-rays refracted by a larger angle (approximately as ± 0.5 FWHM) will be reflected more.

Several physical processes, such as absorption, scattering coherent and incoherent, as well as refraction, are generated while the object is penetrated by X-ray [5]. The X-ray selected by analyser crystal at different angular points of RC will then provide different information on tissues, especially on their interfaces. That means the image obtained with a detuned analyzer crystal will include the information of absorption, scattering and refraction effects. By combining the images taken on either side of the RC, the effects can be separated to get the so-called pure absorption image and the pure refraction image, which show different contrast because of their different contrast mechanisms [4, 5].

All the following experimental procedures of imaging scans are carried out as follows:

1) Acquisition of XACI of specimen

For each specimen, an XACI was taken by moving the analyzer out of the beam and scanning the CCD and specimen through the fan X-ray beam in the same direction and at the same speed.

2) Acquisition DEI images of specimen

The specimens were placed between two crystals, and the distance between them and CCD was about 30 mm. The angle resolution of the analyzer crystal movement was about 0.05 seconds. The analyzer crystal was rotated continuously to adjust the angle of light and to obtain the characteristic RC of each specimen. The DEI images were acquired with the analyzer tuned respectively to the 3 different positions on the RC by penetrating the specimen and CCD in opposite directions at the same speed through the fan beam.

3) The extraction and separation of DEI information

The imaging normalization was carried out with the data of background RC. Of them, the images taken on the ±0.5 FWHM positions of RC were processed digitally by the arithmetic way of pixel to pixel, with which two kinds of new images (refraction image and pure absorption image) were obtained indirectly [5]. As to the peak image it was not necessary to conduct special processing because the analyzer crystal has been tuned to the top of RC when imaging.

After the DEI experiments, the specimens were treated with the routine procedures of alcohol dehydration and paraffin embedding, and were cut to the consecutive slices of 5 μm thick, and then were stained with the hematoxylin-eosin (HE) conventionally. The microscope photos of each specimen were taken afterward.

3 Results

With the experimental procedures mentioned in the last section, five types of X-ray images of 7 specimens are obtained from this experiment: the absorption image (XACI), the pure absorption image extracted from DEI images, the DEI image at the peak of rocking curve, the refraction image extracted from DEI images, and the images taken on the ±0.5FWHM position of RC. The images from two of 7 specimens are shown in Fig. 1 and Fig. 2, which are compared with their corresponding pathological images.

The result for the specimen of intraocular neuroblastoma is shown in Fig. 1. Fig. 1(a) and 1(b) are pathologic images with different magnifications. It is clearly seen that a mass of soft tissues is very prominent to corporis vitre from posterior pole of eyeball. Fig. 1(c) is the image of XACI, which illustrates the tumor mass vaguely but without any fine structures observable. Fig. 1(d) is the pure absorption image extracted from DEI images, which illustrates the body of tumor mass relatively more clear and with some fine structures visible. Fig. 1(e) is the DEI image at the peak of RC, which illustrates the tumor body more clearly and more details of the fine structures. In Fig. 1(f), of the refraction image extracted from DEI images, the most informative fine structures of

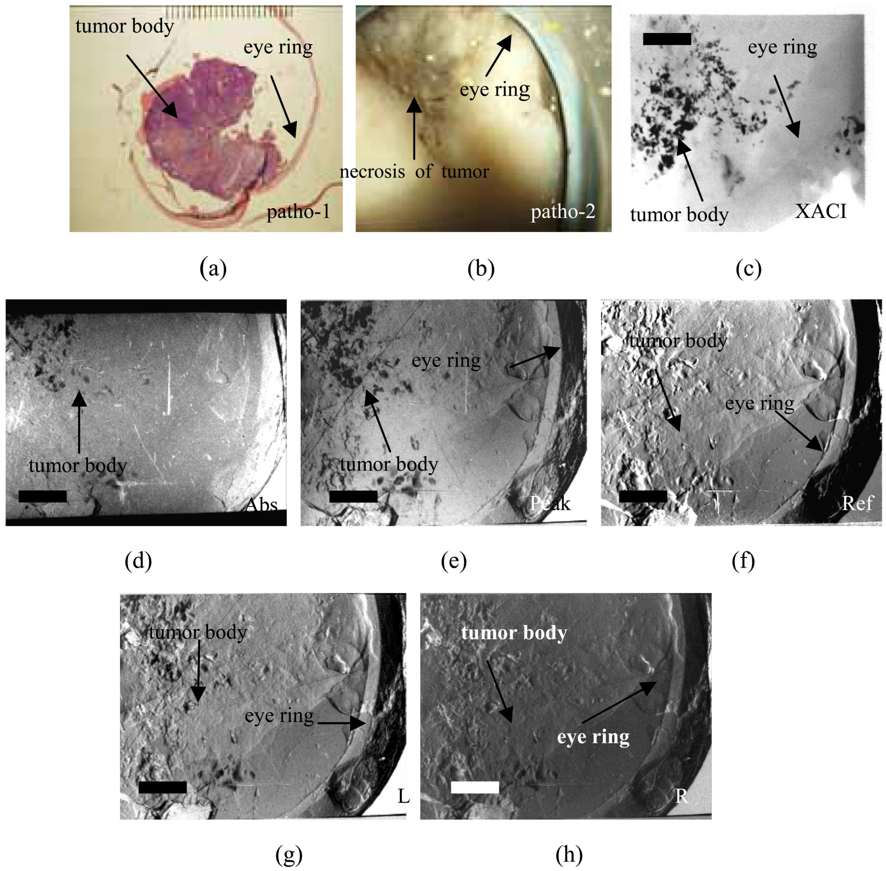

Fig. 1. Images of XACI and DEI compared with the pathology images of specimen intraocular neuroblastoma (scale bar = 2 mm). (a) and (b) Pathologic images with different magnifications; (c) XACI image; (d) Pure absorption image; (e) DEI image at peak of RC; (f) Refraction image; (g) and (h) DEI images at ±0.5FWHM positions of RC.

tumor are displayed. Fig. 1(g) and Fig. 1(f) are the DEI images obtained on the left (L) and right (R) side of the RC, displaying the similar fine structures of tumor mass with those of Fig. 1(d) and Fig. 1(e).

The result for the specimen of the uveal metastatic tumors of intraocular eyeball wall (coronal dimension of the right lower quadrant) is shown in Fig. 2. Fig. 2(a) and 2(b) show the pathologic details of the eye ring, especially the uveal coat is broaden and rather rough in surface. Fig. 1(c) is the image of XACI, which illustrates the eye ring faintly. Fig. 1(d) is the pure absorption image from DEI, which illustrates the thickness of uveal coat in eye ring clearly but with few fine structures. Fig. 1(e) is the DEI image at the peak of RC, and Fig. 1(f) is the refraction image acquired from DEI images, both of them illustrate clearly not only the inner side of eye ring, such as the thickened of uveal coat, but also the fascia and connective tissues outside , as well as the sclera in the middle of eye ring, and their sense of layering is prominent. Fig. 1(g) and 1(f) are the DEI images obtained at ±0.5 FWHM positions of RC illustrating the similar fine structures of eye ring as those of Fig. 1(e) and 1(f).

The image quality obtained in the experiment is mainly evaluated by the way of qualitative visual observation. The criteria used for scoring are comprehensively formulated after discussing together with researchers, radiologists and pathologists. The grade ranging from 0 to 10 is used to remark the pathology and XACI images, and the different grades of classification are from I to V for DEI image quality. Of all grades scorings, the smaller grade number means better image quality. The evaluation was performed by three veteran radiologists who did not know any specific history and details of the experiment. At first, two of the primary radiologists independently reviewed the images and made their own judgments. In the case of disagreement which happened in separate judgments, the third radiologist provided an independent interpretation that served as the tiebreaker [13]. The final evaluation results of

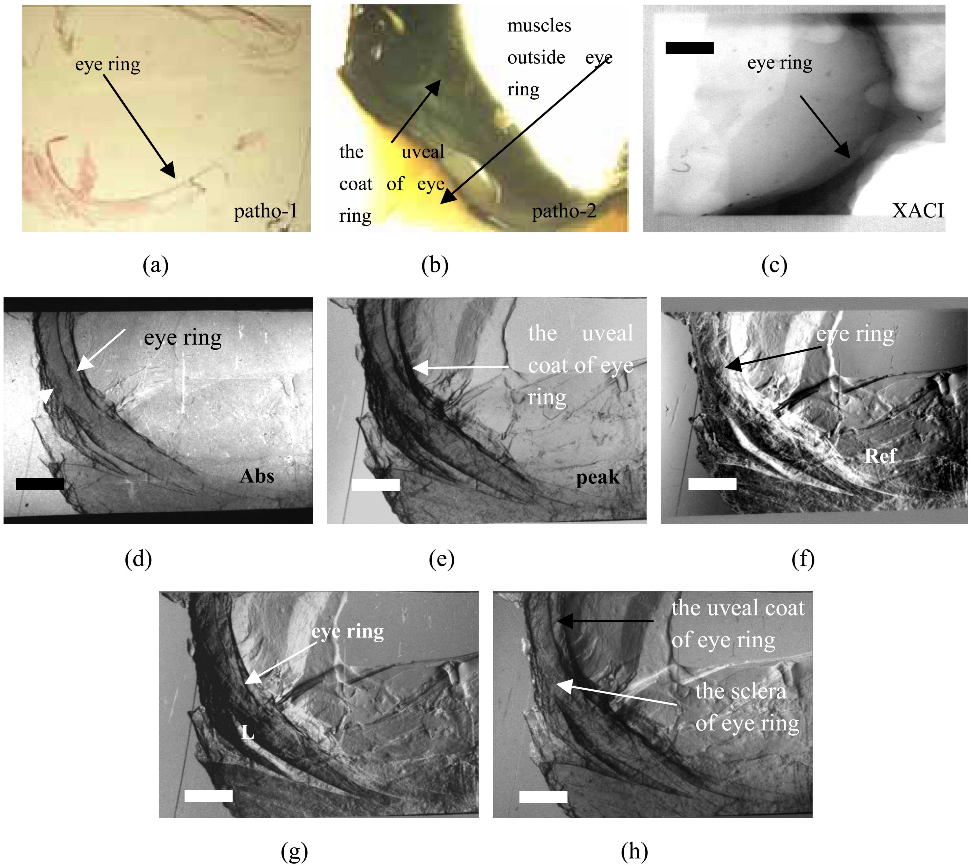

Fig. 2. Images of XACI and DEI compared with the pathology images of specimen of the uveal metastatic tumors of intraocular eyeball wall (coronal dimension of the right lower quadrant). (scale bar = 2 mm) (a) and (b) Pathologic images with different magnifications; (c) XACI image; (d) Pure absorption image; (e) DEI image at peak of RC; (f) Refraction image; (g) and (h) DEI images at ±0.5FWHM positions of RC.

Table 1. Scores grade of images by comprehensive visual observation.

imaging mode / imaging specimen	XACI	DEI					pathology
		left	peak	right	absorption	refraction	
intraocular malignant melanoma 1	X	II	II	II	IV	II	0
intraocular malignant melanoma 2	X	II	III	II	III	I	0
intraocular neuroblastoma	X	II	III	III	IV	II	0
intraocular uvea metastatic –							
right lower quadrant	X	II	II	II	II	II	0
right upper quadrant	X	II	II	II	I	II	0
left upper quadrant	X	II	III	II	III	III	0
left lower quadrant	X	II	II	II	II	I	0
total	70	14	17	15	19	13	0

all the images of all the 7 specimens are listed in Table 1.

As shown in Table 1, the score grades of III or II, some even I are given to most of the DEI images, and in contrast, only the score grade of X is given to all XACI images. It indicates that the difference of image quality between DEI and XACI is significant, and that the image quality of DEI is excellent and what they have shown is very closer to the findings of pathology. Also as shown in Table 1, within the group of DEI, the score grades of image quality are the highest for the refraction images and the lowest for the absorption ones, since most score grades for the former are I or II whereas for the latter are II or III. Furthermore, there are no significant differences of image quality among the left, peak, right and refraction images. It clearly indicates that the images containing refractive information, such as indexed as refraction, left, peak, and right in Table 1, show better image quality than that of the absorption images indexed as XACI in Table 1, and even that of the pure absorption images taken from the DEI experiments indexed as absorption in Table 1.

The edge visibility (V) is a quantitative measurement for image quality evaluation normally adopted in the study of the DEI images after digital transformmation, which is defined and calculated as the following equation [14]:

$$V=\frac{I_1-I_2}{I_1+I_2}, \tag{1}$$

where, I_1 and I_2 are the digital values of gray scale measured with ImageJ1.37v Preferences program on either side of an edge along a line crossing the edge. We also measured the values of edge visibility for each specimen, and four regions of interest (ROI) were chosen in each image to calculate the contrast respectively, in order to check the evaluation results of visual observation. On the other hand, after transforming the image gray into digital data, it is very easy to get the spatial resolution of the image.

As a preliminary and auxiliary result, the spatial resolution and the best edge visibility in the peak image from the specimen of left lower quadrant is measured as about 40 μm and about 0.8, respectively. These data give strong evidence to support the truth that the DEI is a very promising method to observe the microstructures of human eyeball.

4 Discussion

In the ophthalmology, it is quite necessary that the anatomic and pathologic details of the eyeball are discriminated accurately to make a diagnosis early. However, eyeball is a so delicate organ inside human body that until now it is still a difficult task for all of noninvasive medical devices to display its anatomical and tissues details. It is reported that the eyeball specimens from animals of one porcine and one Persian cat were investigated with DEI by two groups of scientists in 2007 and 2008 [11,12]. As to our knowledge, none of the intraocular tissues from human beings has ever been observed with DEI technique before.

As shown in Figs. 1 and 2, it seems possible using the DEI method to display the micro changes of human eyeball, but the micro changes can not to be displayed with the XACI method.

In principle, the behavior of X-rays as they pass through a specimen can be described using a complex index of refraction n, just as in conventional optics.

$$n=1-\delta-\mathrm{i}\beta. \tag{2}$$

The real part δ determines the phase shift of the X-ray when passing through the sample, while the imaginary part β is correlated with the linear absorption coefficient μ [6, 7, 15]. The ratio of δ to β for the light Z elements is normally as large as 1000 in the range of dozens-keV of X-rays. A full understanding of the mechanism underlying the DEI process demands that hard X-rays be treated as waves rather than rays [8]. The phase changes of the X-ray wave cause transverse shifts in the original beam direction (refraction) upon propagation through the media of varying refractive index, which can result in an intensity change in the image plane. Therefore, the refraction image, being sensitive to the gradient of the refractive index, shows dramatic edge enhancement and provides a picture of the boundaries between regions with different refractive indices.

The results of this study show that the XACI images are ambiguous and far from the findings of pathology, and not helpful to the diagnosis. The reason is that the mechanism of XACI is mainly from the photoelectric absorption, and the medical specimen of eye ring and most lesions of the eyeball, and especially the tumors in early stage, are tiny masses of soft tissue with inhomogeneous density made of low Z elements, thus their X-ray absorption attenuation is feeble.

Contrary to the absorption contrast, there is relatively a great amount of phase information in the specimens of eyeball when X-ray penetrates through, which provides the ability to display the eyeball microscopic by the multi-contrast of DEI with synchrotron radiation X-ray. From the results shown above, the neuroblastoma (RB) (Fig. 1) which appeared as a mass of soft tissues was very prominent to corporis vitre from the posterior pole of eyeball. The uveal metastases appeared as the eyeball wall was thickened, but the boundary within the eye ring was not clear (Fig. 2). In particular, most details of the micro-layers of eye ring except the retina, namely the fascia and connective tissue outside the sclera and the uveal coat inside, are all displayed only by the DEI images but not by the XACI images at all.

The image quality of intraocular tumor with DEI technique is constrained by some factors. According to the theory developed [2, 16], the X-ray beam divergence, the quality of the crystals, and the resolution of the CCD detector are the key factors which determine the image quality and the image resolution. Although the DEI image quality in this preliminary study is not yet at the same level as that of the optical microscopy, the thick specimen of 2–5 mm is observed. This will avoid the complex cutting procedures when the optic microscope is used to make the conventional pathologic observation. It is also expected that there are still many possibilities to get a better DEI image quality with future improvements of DEI apparatus, and optimization of the experiment setup [17].

5 Conclusions

In conclusion, the DEI method is used for the first time to display the layers of eye ring and pathology of intraocular tumor in human beings with a resolution of 40 μm. The tiny internal density differences of the eyeball itself and the malignant intraocular tumor which is composed mostly of low Z lighter elements can be observed clearly. There is a great possibility for DEI to be a new micro-imaging method for the eyeball investigation. However, before the clinical trials of DEI method are performed, the data of more extensive conditions with DEI should be accumulated.

This work was completed at the XPCI Platform of 4W1A Topography & Imaging Station of BSRF. The authors also wish to thank Zhao Tian-De and Pan Lin from the Institute of Clinical Medicinal Research, and Sino-Japanese Friendship Hospital in Beijing, for their scientific assistance before and during the experiment, and Huang Wan-Xia at BSRF for the technical support.

References

1 Wagner A, Aurich M, Stoessel M, Sieber N, Wetze W D, Mollenhauer J, Schmuck K, Muehleman C, Lohmann M, Reime B, Metge J, Coan P, Bravin A, Arefelli F, Rigon L, Menk R H. Proceedings of SPIE, **5746**: 542–549

2 Davis T J, GAO D, Gureyev T E, Stevenson A W, Wilkins S W. Nature, 1995, **373**: 595–598

3 Wilkins S W, Gureyev T E, GAO D, Pogany A, Stevenson A W. Nature, 1996, **384**: 335–338

4 Chapman D, Thomlinson W, Johnstonk R E, Washburn D, Pisano E, Gmur N, ZHONG Z, Menk R, Arfelli F, Sayers D. Phys. Med. Biol., 1997, **42**: 2015–2025

5 Chapman D, Pisano E, Thomlinson W, ZHONG Z, Johnstonk R E, Washburn D, Sayers D, Mainowska K. Breast Diseases, 1998, **10**(3,4): 197–207

6 Brain A. J. Phys. D: Appl. Phys., 2003, **36**: A24–A29.

7 Lewis R A, Hall C J, Hufton A P, Evans S, Menk H, Arfelli F, Rigon L, Tromba G, Dance D R, Ellis O, Evans A, Jacobs E, Pinder S E, Rogers K D. The British Journal of Radiology, 2003, **76**: 301–308

8 Yoon C Y, Sung D J, Lee J H, Kim A R, Oh C W, Je J H, Weon B M, Seol S K, Pyun A, Hwu Y, Margaritondo G, Joos K J, Yoon D K. Int. J. Urol., 2007, **14**: 96–103

9 Bravia A, Kerylainen J, Ferandez M, Firdler S, Nemoz C, Karjalainen-Lindsberg M L, Tenhunen M, Virkkunen P, Leidenius M, Smitten K, Sipila P, Suortti P. Phys. Med. Biol., 2007, **52**: 2197–2211

10 Lewis R A. Phys. Med. Biol., 2004, **49**: 3573–3583

11 Keely M E, Coupali D J, Beavans R C, Schultke E, Romanchuk K, Juurlink B H J, ZHONG Z, Chapaman L D. Can J Ophthalmology, 2007, **42**: 731–733

12 Honnickea M G, Cusatisa C, Antunesb A, Safatle A M V, Barros P S M, Morelhao S L. Nuclear Instruments and Methods in Physics Research A, 2008, **584**: 418–423

13 YU Yong-Qiang, XIONG Zhuang, LÜ Yi-Zhong, QIAN Yin-Feng, JIANG Shi-Ping, TIAN Zhuang. Skeletal Radiol, 2006, **35**: 156–164

14 Pagot E, Fiedler S, Cloetens P, Brain A, Coan P, Fezzaa K, Baruchel J, Hartwig J. Phys. Med. Biol., 2005, **50**: 709–724

15 Subonen H, Fernandez M, Bravin A, Keryilainen J, Sourtti P. Synchrotron Rad., 2007, **14**: 512–521

16 Lewis R A, yagi N, Kitchen M J, Morgan M J, Paganian D, Siu K K W, Palov K, Williams I, Uesugi K, Wallace M J, Hall C J, Whitley J, Hooper S B. Phys. Med. Biol., 2005, **50**: 50311-5041

17 Crittella S, Ibisona M, Cheungb K C, Hodgson R, Gould D, Hall C, Nolan P J, Page R D. Nuclear Instruments and Methods in Physics Research A, 2007, **580**: 1131–1133